3D MHD models of colliding-wind binaries

K. Reitberger, R. Kissmann, A. Reimer, and O. Reimer

Institute for astro & particle physics

Universität Innsbruck

Variable Galactic Gamma-Ray Sources (IV)

July 6th 2017

Rikkyo University (Tokyo)

Contents

1. introduction to colliding-wind binaries (CWBs) in γ rays
2. model framework
3. results on γ^2 *Velorum* (WR 11)
4. η Carinae, WR 140, and γ^2 Velorum – a comparison
5. Summary & outlook

Particle-accelerating colliding wind binaries

- massive systems of 2 or more stars (OB, WR, LBV)
- collision of stellar winds with high momenta
- wind-collision region (WCR) bound by shocks
- leptonic and hadronic populations of high-energy particles
- ability to compute nonthermal emission via synchrotron, inverse Compton (IC), bremsstrahlung and π^0 decay channels.

Example of a simulation showing stellar wind-velocity and number density of high-energy protons @ 20 GeV

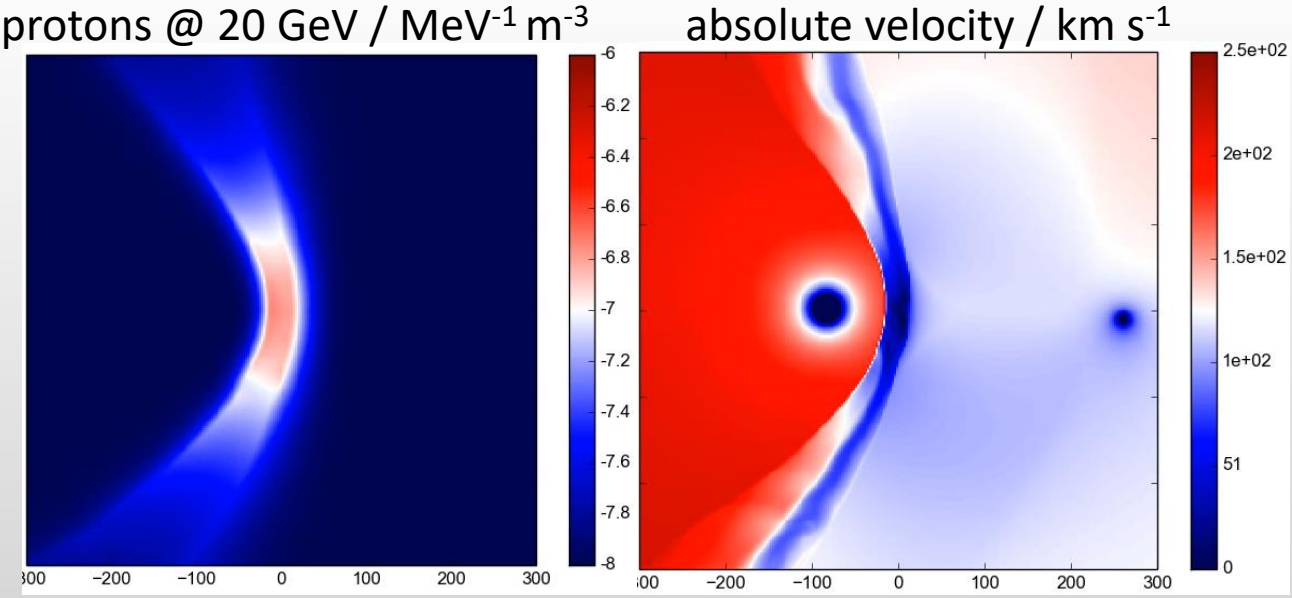

Particle-accelerating colliding wind binaries

- 43 suspected systems (see catalogue by de Becker and Raucq 2013)

- 42 characterized by evidence for nonthermal radio emission.

  → Plausible cause: synchrotron emission of high-energy electrons in stellar magnetic fields

- only 2 systems show evidence of high energy γ-ray emission (η Carinae & γ^2Velorum)

- Interesting mismatch between theoretical predictions and non-detection at high-energies for some other systems (e.g. WR 140, WR 147).

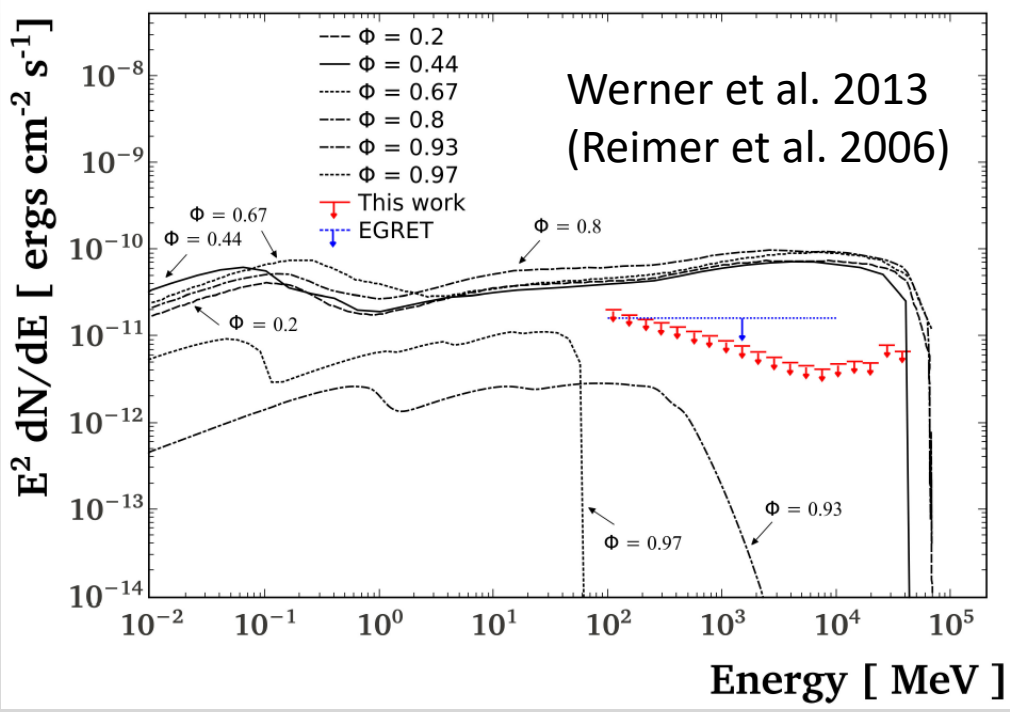

3 very different CWB systems

	γ^2 Vel	η Car	WR 140	
period	~ 80[5]	~ 2024[3]	~ 2900[7]	d
eccentricity	$\sim \mathbf{0.3}$[6]	$\sim \mathbf{0.9}$[1]	$\sim \mathbf{0.9}$[7]	
distance	$\sim \mathbf{340}$[6]	$\sim \mathbf{2300}$[2]	$\sim \mathbf{1800}$[8]	pc
stellar separation	$170 - 340$	$330 - 6300$	$360 - 6700$	$R_\odot$
mass loss primary	~ 2[5]	$\sim \mathbf{2500}$[4]	~ 90[5]	$10^{-7}\ M_{sol}\ y^{-1}$
dominant wind	secondary (WR)	**primary (LBV)**	secondary (WR)	

Reference

1 Smith et al. 2004
2 Davidson & Humphreys 1997
3 Corcoran et al. 2005
4 Pittard & Corcoran 2002
5 van der Hucht 2001
6 North et al. 2007
7 Marchenko et al. 2003
8 Dougherty et al. 2005

3 very different CWB systems

	γ^2 Vel	η Car	WR 140	units
Spectral type	WC8 + O7.4	WR? + LBV	WC7 + O8	
Total kinetic power of wind	$\mathbf{0.6}$[1]	$\mathbf{2.8}$[3]	$\mathbf{6.1}$[3]	10^{37} erg s^{-1}
High-energy γ-ray flux (0.1 to 100 GeV)	$\mathbf{1.8} \pm 0.6$[1]	$\mathbf{184} \pm 30$[2]	$< \mathbf{1.1}$[1] / < 9.6[4]	10^{-9} ph cm^{-2}s^{-1}
Orbital modulation	no[1]	yes[5]	-	
γ-ray luminosity	0.0037[1]	$\mathbf{7.8}$[2]	-	10^{34} erg s^{-1}
nonthermal radio luminosity	1.5[3]	-	26[3]	10^{29} erg s^{-1}

1 Pshirkov 2016
2 Fermi LAT 4-Year Point Source Catalog
3 De Becker et al. 2013
4 Werner et al. 2013
5 Reitberger et al. 2015

The model – brief overview …

- 3D MHD code
  - radiative line-acceleration to generate stellar winds
  - B-field determined by choice of stellar surface-magnetic field
  - radiative cooling considered

The model – brief overview …

- 3D MHD code
  - radiative line-acceleration to generate stellar winds
  - B-field determined by choice of stellar surface-magnetic field
  - radiative cooling considered

- 200 advected scalar fields representing $\boldsymbol{e^-}$ and $\boldsymbol{p}$ at different energy bins
  - solution of transport equation for each computational cell and time steps

$$\underbrace{\frac{\partial j}{\partial t}}_{(1)} - \underbrace{D(E)\nabla^2 j}_{(1)} + \underbrace{\nabla \cdot (\vec{u} j)}_{(2)} - \underbrace{\frac{\partial}{\partial E}\left[\left(\frac{E}{3}\nabla \cdot \vec{u} + \dot{E}_{\text{loss}}\right) j(E)\right]}_{(3)} = \underbrace{Q_0 \delta(E - E_0)}_{(4)}$$

1) spatial diffusion with $D = D_0 E^{\delta}$
2) spatial convection
3) energy gains and losses
4) particle injection at E_0

Our model – brief overview …

- 3D MHD code
  - radiative line-acceleration to generate stellar winds
  - B-field determined by choice of stellar surface-magnetic field
  - radiative cooling considered

- 200 advected scalar fields representing $\boldsymbol{e^-}$ and $\boldsymbol{p}$ at different energy bins
  - solution of transport equation for each computational cell and time steps

- γ-ray emission components are computed from particle spectra and surrounding conditions (radiation + magnetic field, wind plasma)
  - inverse Compton
  - bremsstrahlung
  - π^0-decay
  - attenuation by photon-photon absorption

Results of modelling γ^2Velorum

#1 In contrast to earlier simulations (e.g. Henley et al. 2005) , we are the first to model the wind of γ^2Vel with a **large shock-cone opening angle**. This is **observed** by X-ray spectroscopy.

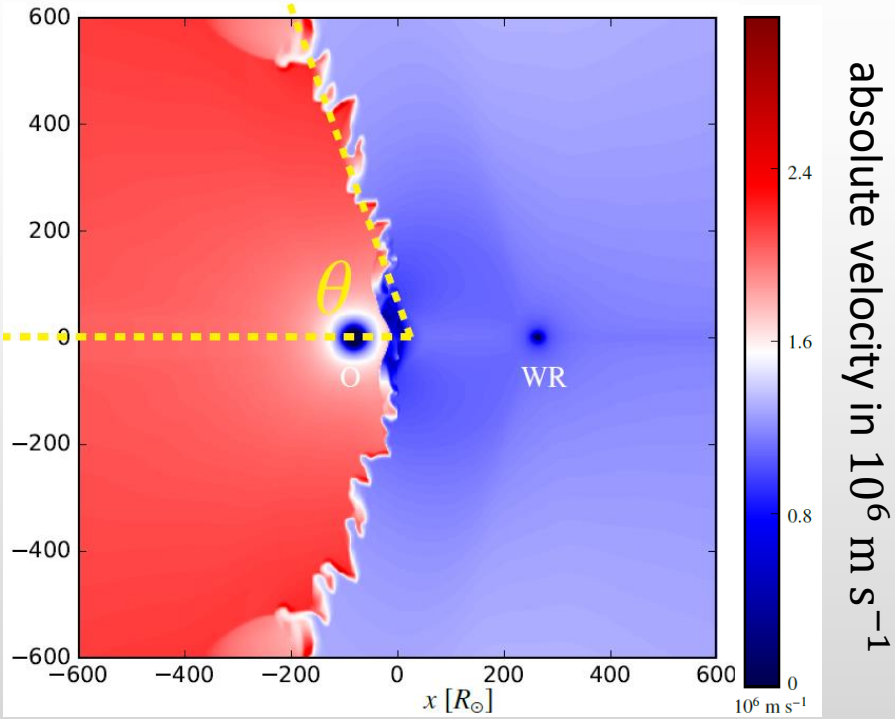

(K.R. et al. in submission)

Results of modelling γ^2Vel

#2 Owing to severe energy loss of the electrons by inverse Compton cooling (and synchrotron emission), γ^2Vel is a clear case of hadronic dominance in the high-energy γ-ray emission.

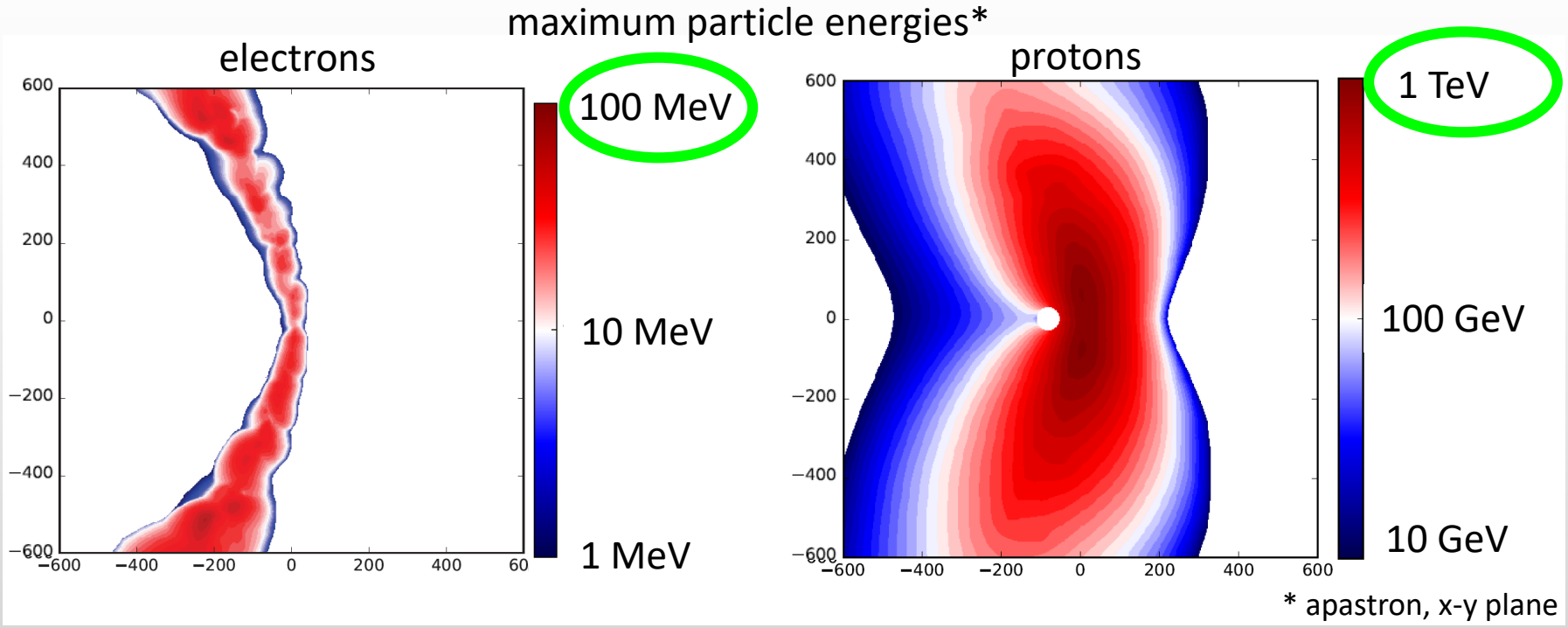

Results of modelling γ^2Vel

#3 We see significant variability on orbital timescales. Periastron conditions are much less favourable for the acceleration of protons due to lower wind speeds and smaller volume of the collision region.

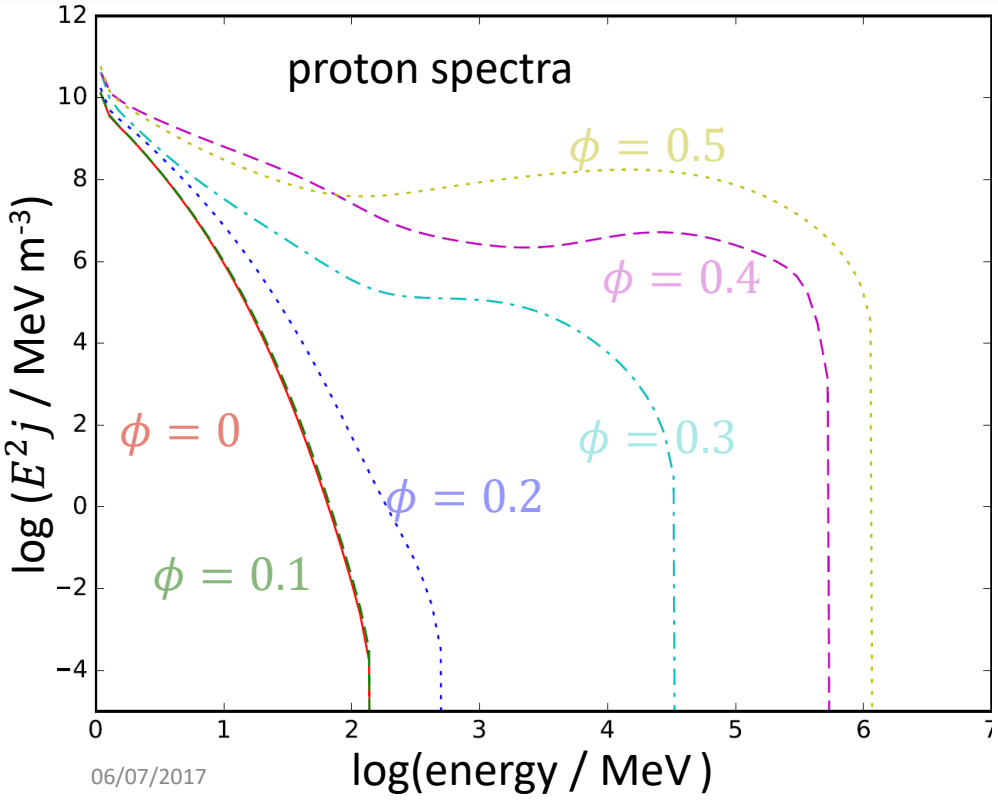

phase	stellar separation	max. proton energy
0.5	344	1 100
0.4	314	520
0.3	259	33.0
0.2	208	0.50
0.1	181	0.14
0	172	0.14
	$R_\odot$	GeV

Results of modelling γ^2Vel

#4 Two important free parameters to alter/fit proton spectra (& nonthermal photon emission) spectra are:

- **particle injection ratio η_p**
- **diffusion coefficient normalization D_0** $\left(D(E) = D_0 \left(\frac{E}{1\text{MeV}}\right)^{\delta}\right)$

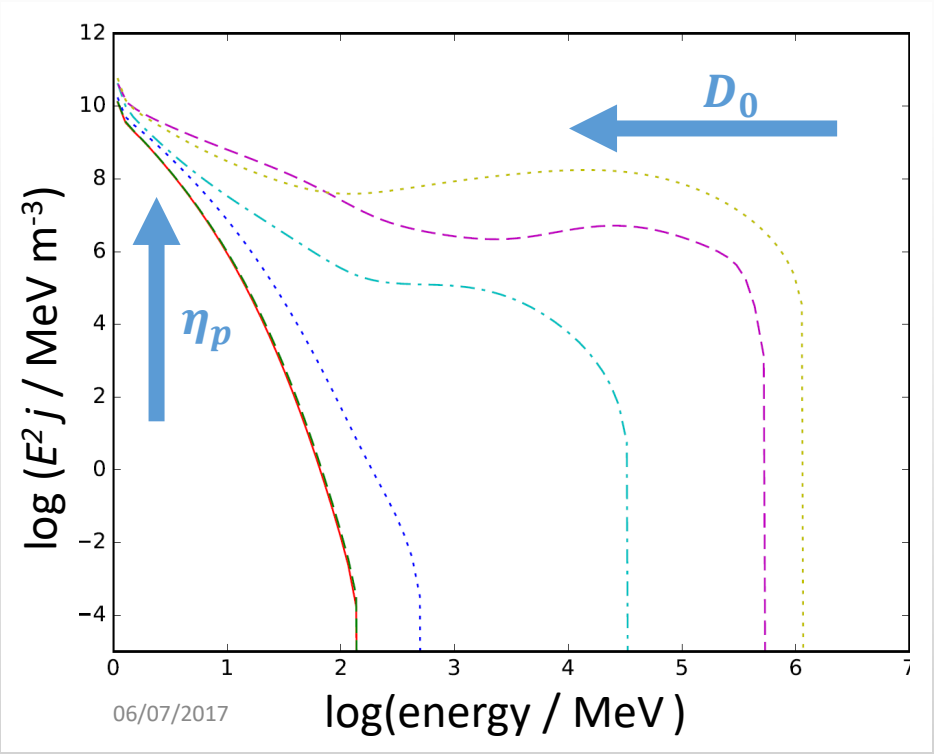

Simulations match the observed *Fermi*-LAT data for

phase	η_p	D_0
0.5	10^{-3}	8×10^{14}
0.4	3×10^{-3}	5×10^{14}
0.3	6×10^{-3}	3×10^{14}
0.2	~1	-
0.1	>1	-
0	>1	-
-	-	$m^2 s^{-1}$

Results of modelling γ^2Vel

#5 The *Fermi*-LAT data can be brought into agreement with the model in the orbital range 0.5 to 0.3 for a reasonable set of parameters η_p and $D_{0.}$

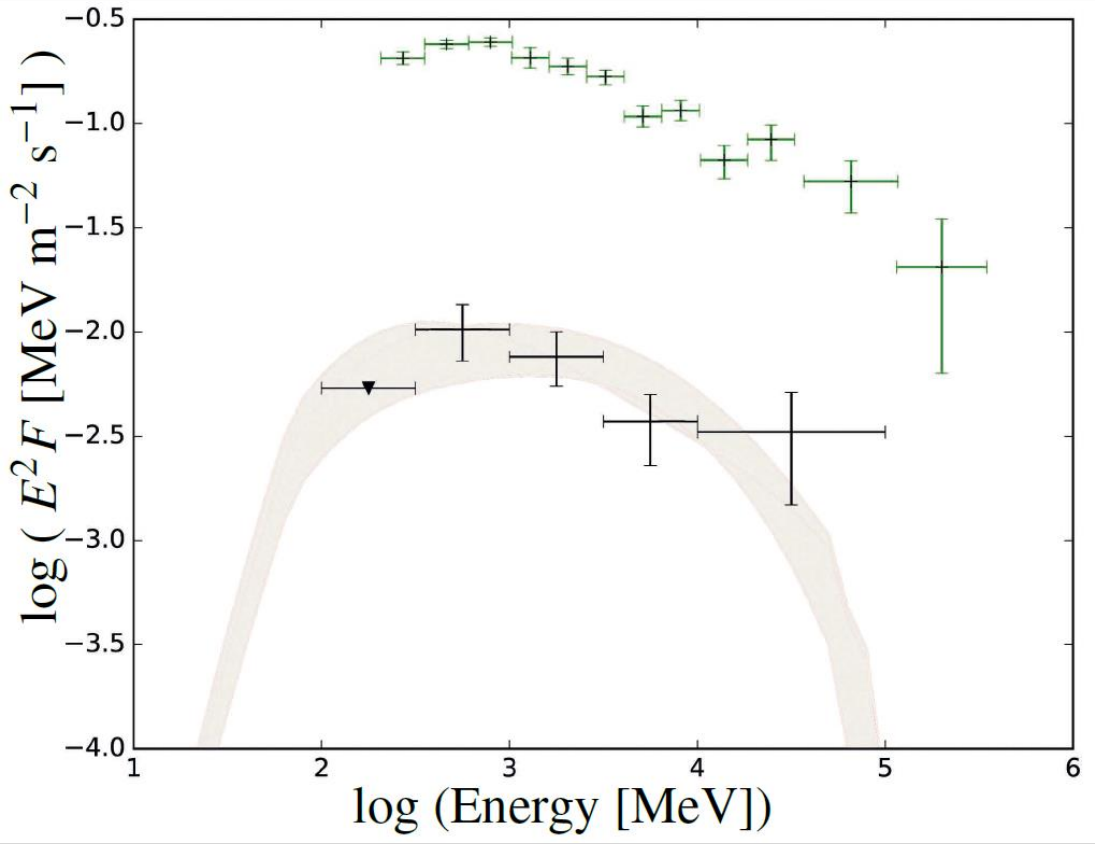

black: *Fermi*-LAT data of γ^2 *Velorum* (Pshirkov 2016)

grey-shaded: range of simulation results

green: *Fermi*-LAT data of η *Carinae* (Reitberger et al. 2015)

Results of modelling γ^2Vel

#6 Most of the γ-ray emission from π^0-decay has its **origin at the apex** of the wind-collision in a region roughly 0.01 arcsec ($\sim$**700** $\boldsymbol{R_\odot}$) wide.

projected Flux > 100 MeV of nonthermal photons from π^0-decay*

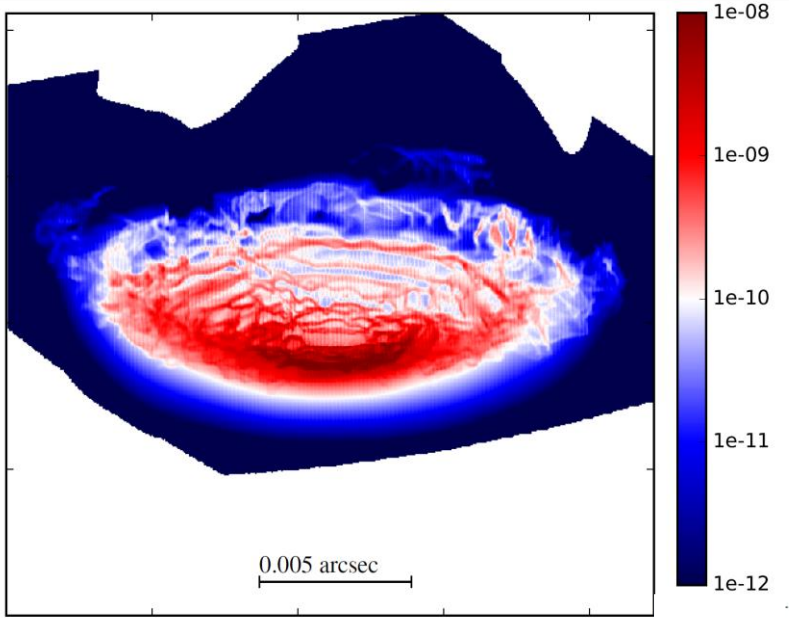

$\mathrm{ph\ m^{-2} s^{-1}}$

* at apastron

line-of-sight: $i = 65° \pm 8°$, $\Phi = 68° \pm 4°$

(Schmutz et al. 1997)

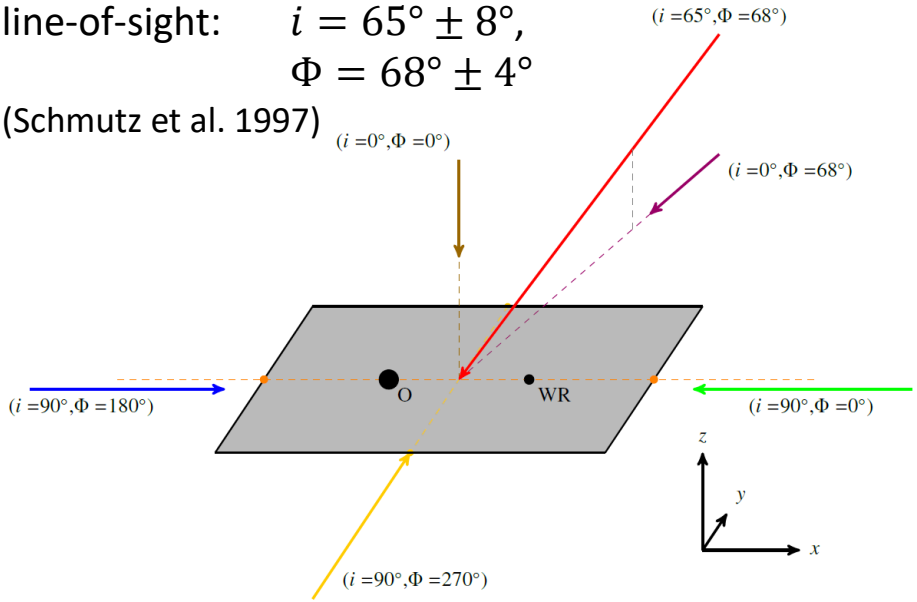

Results of modelling γ^2Vel

#7 Comparison of leptonic and hadronic emission components.

Data points and upper limits:

for γ^2Velorum:
ASCA (blue)
Integral/IBIS (red)
Tatischeff et al. 2004

Fermi-LAT (black)
Pshirkov 2016

for η Carinae:
Fermi-LAT (green)
Reitberger et al. 2015

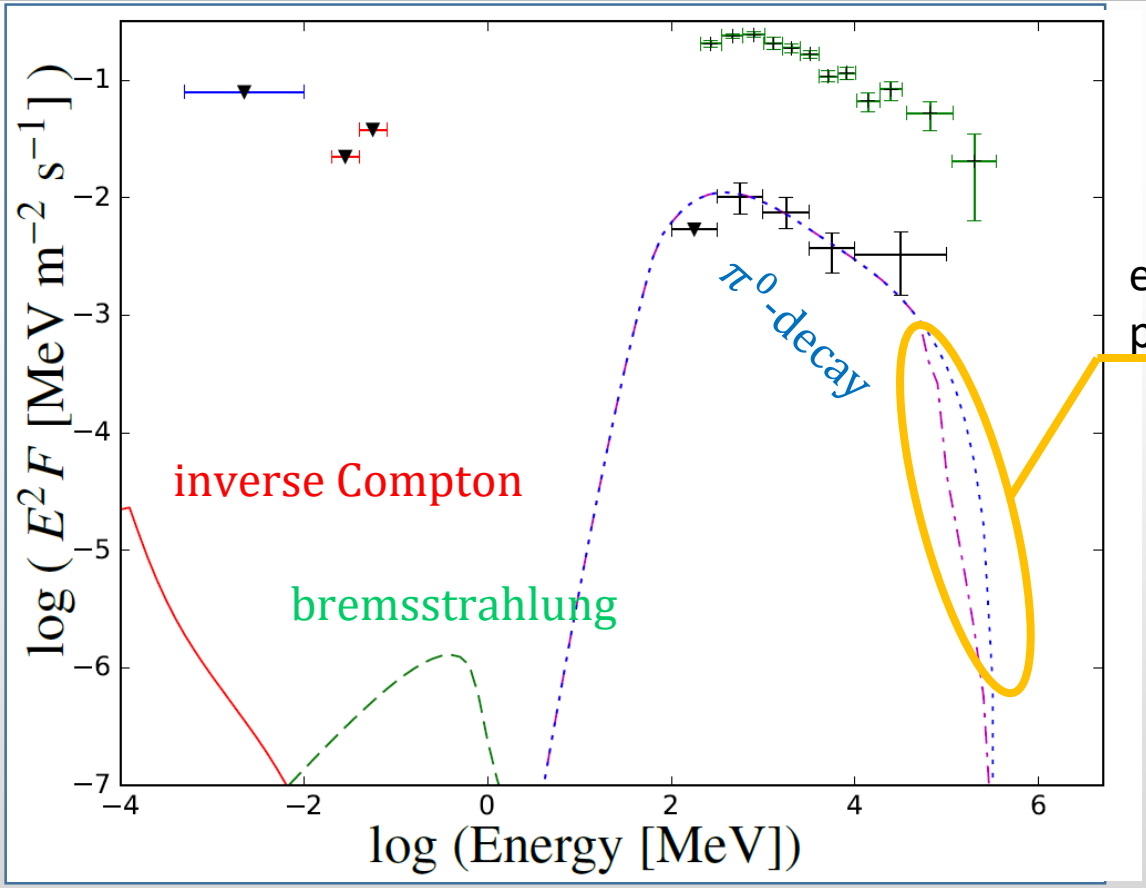

Summary of γ^2Velorum results

- agreement of wind-structure with observations
- leptonic γ-ray emission highly unlikely
- orbital variability expected: lower γ-ray emission near periastron
- small emission region ($\sim 700\ \mathrm{R}_\odot$) of hadronic γ-ray emission
- constraints on mass-loss rate of secondary star
- observed and simulated SEDs agree

Now: application to η Car and WR 140

Wind plasma density @ apastron

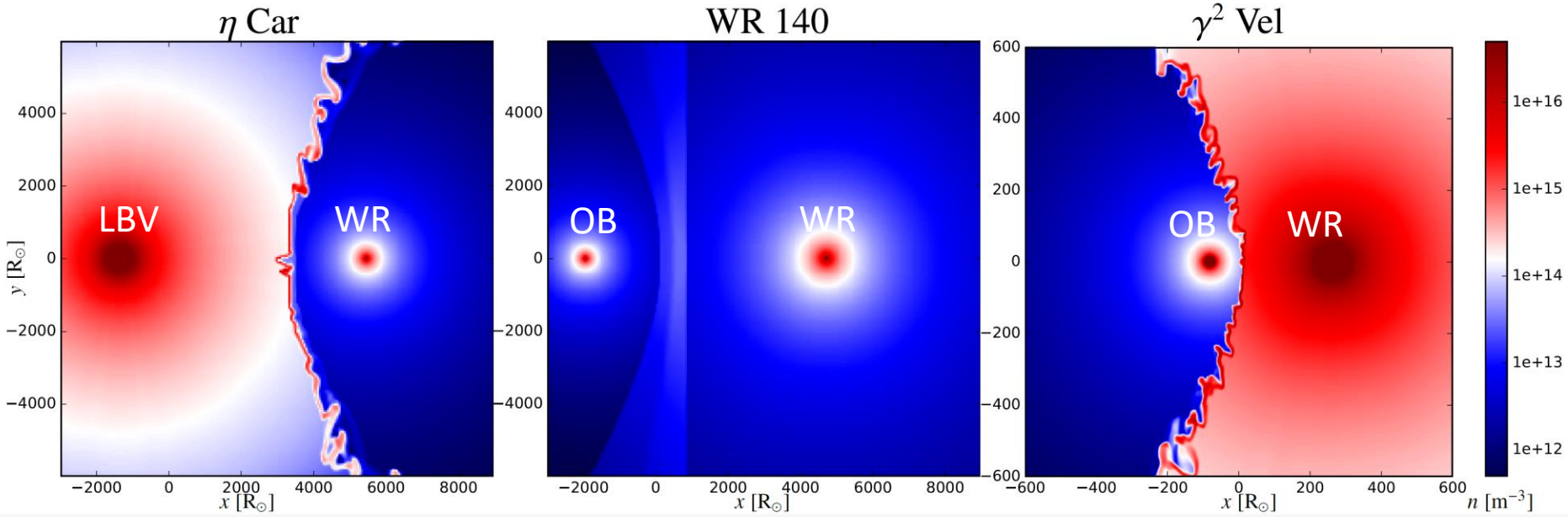

	ηCar	WR 140	γ^2Vel	
box width	12	12	1.2	10^3 $R_\odot$
Maximum density in WCR	$\mathbf{1 \times 10^{16}}$	$\mathbf{3 \times 10^{13}}$	$\mathbf{9 \times 10^{16}}$	m^{-3}
Apex wind velocity WR wind	2900	2800	1300	km s^{-1}
Apex wind velocity OB/LBV wind	540	3000	2000	km s^{-1}
Maximal temperature in WCR	1.1	1.4	0.6	10^8 K

The significance of wind plasma density n_H

n_{H} influences the computation of final results at two points:

- particle injection at E_0: $\mathrm{Q}_0 = \eta_{p,e} \boldsymbol{n_{\mathrm{H}}} \frac{1}{(1+4\zeta_{\mathrm{He}})}$
- pion production: $\frac{dn_{\pi^0}}{dE_\pi}(E_\pi) = c\boldsymbol{n_H}\sigma_{pp}^{\pi}\left(m_p c^2 + \frac{E_\pi}{K_\pi}\right)\frac{dn_p}{dE_p}\left(m_p c^2 + \frac{\mathrm{E}_\pi}{K_\pi}\right)$

(following Kelner et al. 2006)

naïve expectation: At a given proton energy, the resulting nonthermal photon flux F from π^0decay depends on the square of wind plasma density.

$$\frac{dF_{\pi^0\mathrm{decay}}}{dE_\gamma} \propto n_{\mathrm{H}}^2$$

Not true! → neglecting loss rates, diffusion, volume of emission region etc.

Particle results

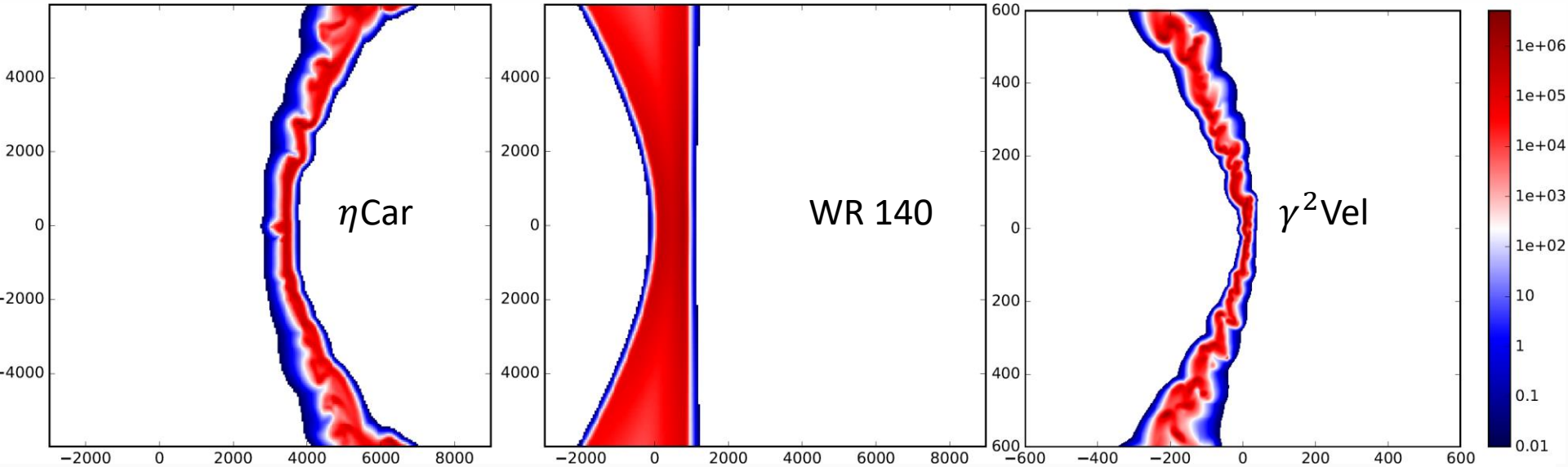

Proton density @$E \sim 1$ MeV

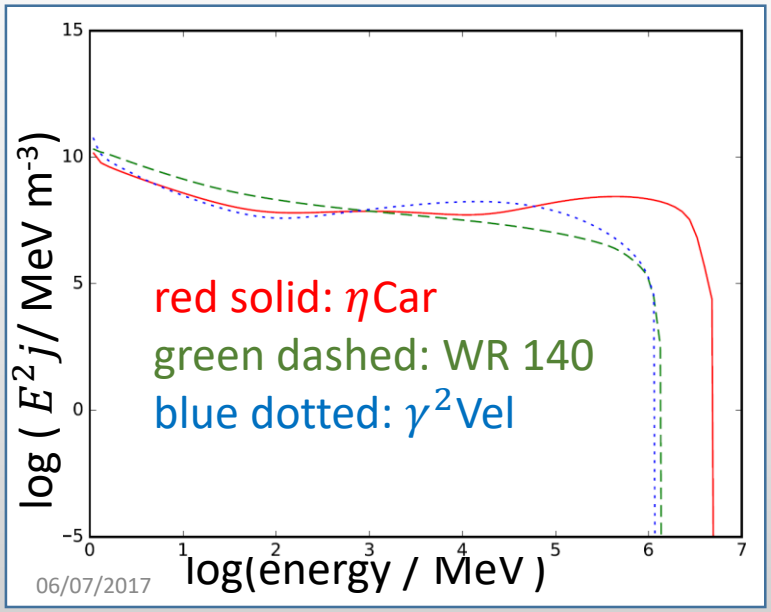

Only minor difference in maximum energy and/or maximum particle density!

Main reasons:

1. WR 140 has WCR with larger volume
2. WR 140 has higher $\nabla \cdot \vec{v}$ → higher acceleration rate
3. higher n_{H} → higher loss-rates (Coulomb+collision)

cancel out the effect of a higher injection rate on the population of high-energy protons.

γ-ray results

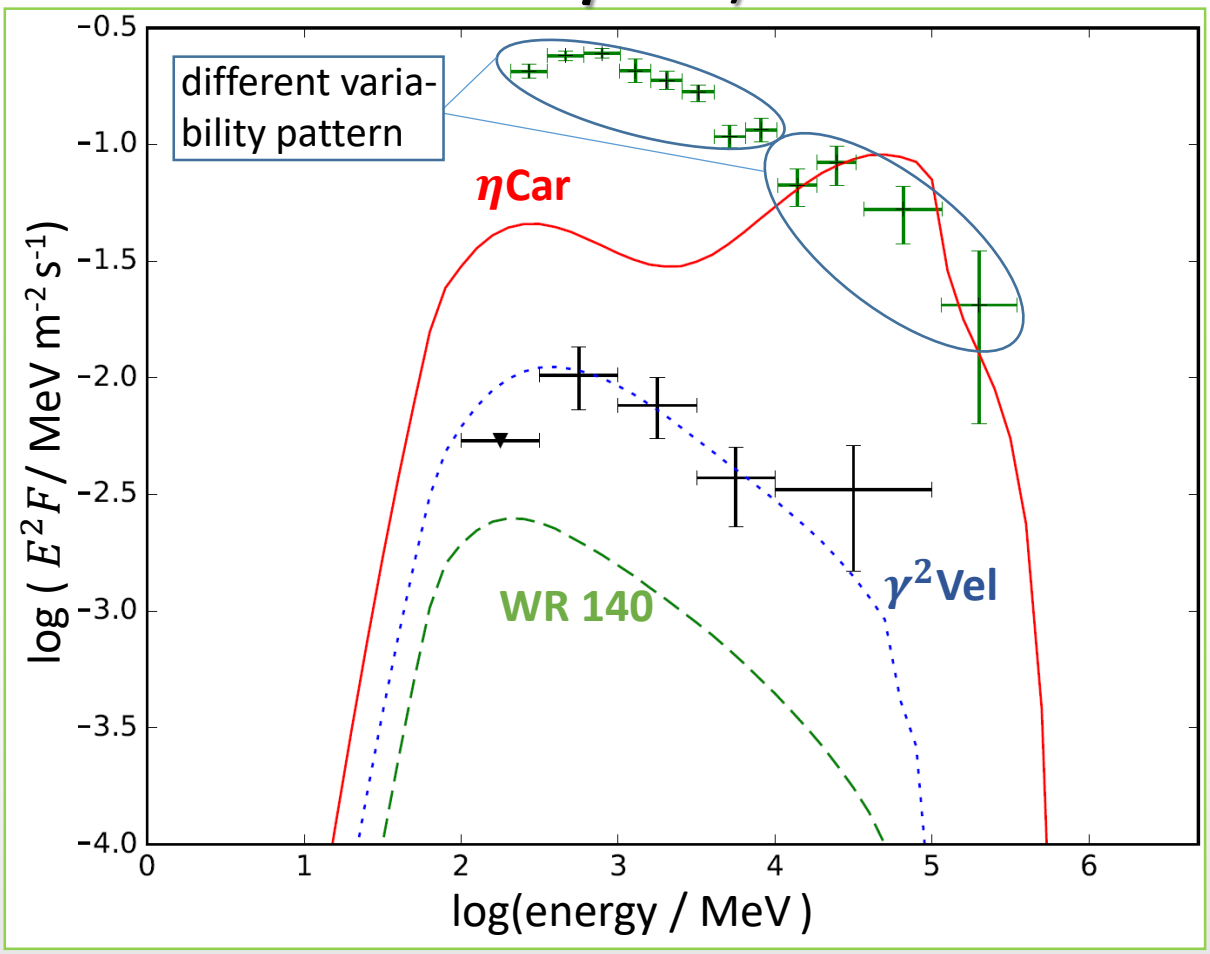

SED with simulated π^0decay components for η Car, γ^2Vel, and WR 140 along with the data points for ηCar from (Reitberger et al. 2015) and for γ^2Vel (Pshirkov 2016).

Here, the huge contrast in plasma density relates to a contrast of flux at about the same order of magnitude.

The simulations for ηCar and WR 140 use exactly the **same resolution**, **same normalization of diffusion**, **same proton injection ratio**, etc. They only differ in the stellar, stellar wind, and orbital parameters!

for both systems: $\eta_p = 4 \times 10^{-3}$ & $D_0 = 1 \times 10^{16}\ \mathrm{m^2 s^{-1}}$

Conclusions

Our simulations reproduce puzzling discrepancies between observations:

1. of the "second emission component" of η Car at $E > 10$ GeV
2. of the non-detection of WR 140

at γ-ray energies

- Keeping all parameters (except stellar, stellar wind and orbital parameters) constant, we simulate emission via the π^0 decay channel that agrees with the measured data for η Car and the upper limits on WR 140.

- The γ-ray emission measured for γ^2Vel can also be accounted for with different values of diffusion normalization and injection ratio.

Outlook

From orbital snapshot to multi-orbital analysis!

→So far the effects of orbital motion (Coriolis force, etc.) have been neglected

comparison with newest observational data!

→*Fermi*-LAT: indications for variability between orbits (Balbo & Walter 2017)

→H.E.S.S. detection

Can the lower emission component of η Car be explained by simulated leptonic γ-ray emission?

→unlikely due to low max. energies of electrons, IC losses very high

→but what if LBV radiation is attenuated in the WR wind by the WCR?

further exploring the MHD-parameter space including the effects of stronger magnetic fields (see Kissmann et al. 2016)

→currently we use rather low surface magnetic field of $B = 10^{-3}$ T